Concerted and Stepwise Dehydration Mechanisms Observed in Wild-Type and Mutated Escherichia coli dTDP-Glucose 4,6-Dehydratase †

ARTICLE *in* BIOCHEMISTRY · MARCH 2002

Impact Factor: 3.02 · DOI: 10.1021/bi011748c · Source: PubMed

3 AUTHORS, INCLUDING:

Adrian Hegeman
University of Minnesota Twin Cities
77 PUBLICATIONS **2,262** CITATIONS
SEE PROFILE

Perry Allen Frey
University of Wisconsin–Madison
302 PUBLICATIONS **10,242** CITATIONS
SEE PROFILE

Concerted and Stepwise Dehydration Mechanisms Observed in Wild-Type and Mutated *Escherichia coli* dTDP-Glucose 4,6-Dehydratase†

Adrian D. Hegeman,‡ Jeffrey W. Gross,‡ and Perry A. Frey*

Department of Biochemistry, University of Wisconsin−Madison, Madison, Wisconsin 53705

Received August 31, 2001; Revised Manuscript Received January 2, 2002

ABSTRACT: The conversion of dTDP-glucose into dTDP-4-keto-6-deoxyglucose by *Escherichia coli* dTDP-glucose 4,6-dehydratase (4,6-dehydratase) takes place in the active site in three steps: dehydrogenation to dTDP-4-ketoglucose, dehydration to dTDP-4-ketoglucose-5,6-ene, and rereduction of C6 to the methyl group. The 4,6-dehydratase makes use of tightly bound NAD^+ as the coenzyme for transiently oxidizing the substrate, activating it for the dehydration step. Dehydration may occur by either of two mechanisms, enolization of the dTDP-4-ketoglucose intermediate, followed by elimination [as proposed for β-eliminations by Gerlt, J. A., and Gassman, P. G. (1992) *J. Am. Chem. Soc. 114*, 5928−5934], or a concerted 5,6-elimination of water from the intermediate. To assign one of these two mechanisms, a simultaneous kinetic characterization of glucosyl C5($^1H/^2H$) solvent hydrogen and C6($^{16}OH/^{18}OH$) solvent oxygen exchange was performed using matrix-assisted laser desorption/ionization time-of-flight mass spectrometry. The reaction of the wild-type enzyme is shown to proceed through a concerted dehydration mechanism. Interestingly, mutation of Asp135, the acid catalyst, to Asn or Ala alters the mechanism, allowing enolization to occur to varying extents. While aspartic acid 135 is the acid catalyst for dehydration in the wild-type enzyme, the differential enolization capabilities of D135N and D135A dehydratases suggest an additional role for this residue. We postulate that the switch from a concerted to stepwise dehydration mechanism observed in the aspartic acid variants is due to the loss of control over the glucosyl C5−C6 bond rotation in the active site.

dTDP-glucose 4,6-dehydratase[1,2] catalyzes the conversion of dTDP-glucose into dTDP-4-keto-6-deoxyglucose. The homodimeric *Escherichia coli* 4,6-dehydratase (RffG) contains one irreversibly bound NAD^+ per subunit and catalyzes a net redox neutral reaction through a mechanism that includes four chemically distinct species (Scheme 1). The first step, 4-dehydrogenation of substrate, is a critical activating step for β-elimination of water between C5 and C6. In the absence of activation by the adjacent ketone group, deprotonation at C5 ($pK_a > 40$) would be impossible under any conceivable conditions in an enzymatic active site. While the 4-keto functionality acidifies the C5 proton, bringing its pK_a into the range of 18−19 (*1*), it also creates additional possibilities for the catalytic mechanism of dehydration. In particular, water elimination might proceed more quickly by enolization to an enol (or enolate) intermediate, as depicted in Scheme 2, than by concerted elimination. In Schemes 1 and 2 NAD^+, NADH, and all dTDP sugars remain bound to the active site throughout the course of a single turnover.

Scheme 1

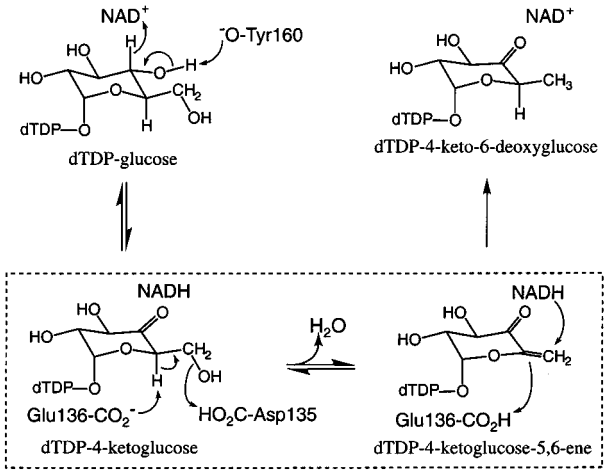

Concerted Water Elimination

In enzyme-catalyzed α-β elimination reactions where activation by the carbonyl functionality may not be sufficient, enol formation with concerted α-proton abstraction and stabilization of the enolate has been proposed to explain the observed rate enhancements (*2*). Certainly such a mechanism presents additional opportunities for enzymatic catalysis, such as protonation of the enolate oxygen, or electrostatic catalysis of the enolate formation. Mechanisms for the 4,6-dehydratase that include an enol/enolate have appeared consistently in the literature, the earliest by Gabriel and Lindquist (*3*) and the most recent by Allard and co-workers (*4*).

A recent study has shown that the 4,6-dehydratase active site contains a base, Glu136, and an acid, Asp135, that

† This work was supported by Grants GM30480 (P.A.F.) and GM20552 (J.W.G.) from the National Institute of General Medical Sciences.

* Corresponding author. Tel: (608) 262-0055. Fax: (608) 265-2904. E-mail: frey@biochem.wisc.edu.

‡ Both authors have contributed equally to this work.

[1] Abbreviations: BSA, bovine serum albumin; 4,6-dehydratase, dTDP-glucose 4,6-dehydratase; dTDP-glucose, thymidine 5′-diphospho-α-D-glucose; dTDP-glucose-d_7, dTDP-[1,2,3,4,5,6,6-$^2H_7$]glucose; DTT, dithiothreitol; MALDI-TOF MS, matrix-assisted laser desorption/ionization time-of-flight mass spectrometry; NAD^+, nicotinamide adenine dinucleotide (oxidized); NADH, nicotinamide adenine dinucleotide (reduced); Tris, tris(hydroxymethyl)aminomethane; wt, wild type.

[2] dTDP α-D-glucose 4,6-hydro-lyase, EC 4.2.1.46.

10.1021/bi011748c CCC: $22.00
Published on Web 01/31/2002

Scheme 2

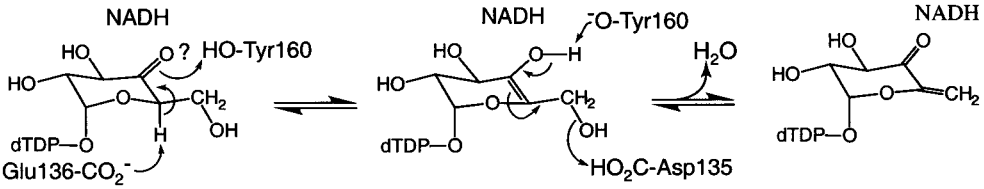

Stepwise Elimination

catalyze dehydration (*5*). While the elimination of water has been shown to proceed with *syn* stereochemistry with respect to the C5(H) and C6(OH) (*6*), no information has been published that would help to distinguish between the concerted and stepwise mechanisms for dehydration outlined in Schemes 1 and 2. It is important for the precise understanding of the function of 4,6-dehydratase that the mechanistic relevance of enolization be determined.

During the 4,6-dehydratase-catalyzed conversion of substrate to product, there is complete exchange of the C5(H) with solvent hydrogen (*3*, *7*). To accomplish this, Glu136 must exchange rapidly with solvent prior to the reprotonation of C5, which occurs in the reduction of the dTDP-4-keto-glucose-5,6-ene by NADH (Scheme 1). This C5(H/D) exchange has also been observed in the absence of net catalysis. In our recent pre-steady-state analysis of wt 4,6-dehydratase *(8)*, using dTDP-glucose-d_7 as the substrate, we observed the transient formation of C5-exchanged substrate (dTDP-glucose-d_6). It became apparent that C5(H/D) and C6-(^{16}OH/^{18}OH) substrate exchange reactions could be used as tools to detect the involvement of an enolate intermediate in the chemistry of water elimination. If water elimination occurs in concert with C5(H) abstraction, then the rates of deuterium exchange at C5 and [^{18}O]water exchange at C6 should be identical. However, if an enol/enolate intermediate forms to any significant extent prior to water elimination, one would expect the rate of solvent hydrogen exchange from C5 to exceed the [^{18}O]water exchange from C6. In this study we present the kinetic analysis of C5 solvent hydrogen (D/H) and C6(^{16}OH/^{18}OH) solvent oxygen exchange into substrate catalyzed by wt 4,6-dehydratase and two Asp135 variants (D135N and D135A dehydratases). In addition to being the acid catalyst for dehydration, active site residue Asp135 has been found to be an important controlling determinant for enolization.

EXPERIMENTAL PROCEDURES

Methods and Materials. wt, D135N, and D135A 4,6-dehydratases were prepared using the affinity purification system and procedure outlined previously (*9*). Synthesis and purification of dTDP-α-D-glucose-d_7 and analysis of samples by MALDI-TOF MS were performed as described previously (*8*). Mass spectra were collected on a PE-Biosystems Voyager-DE MALDI-TOF mass spectrometer, equipped with delayed extraction, in negative reflectron mode. Enzyme and nucleotide sugar concentrations were determined using UV/visible measurements with a Shimadzu UV-1601PC dual beam spectrophotometer and the extinction coefficients 81000 M^{-1} cm^{-1} for enzyme and 10200 M^{-1} cm^{-1} for thymidine nucleotides, both at pH 7.0 and 20 °C.

[^{18}O]Water. A 1 mL sample of [^{18}O]water (~80% enriched and containing HCl) was generously provided by W. W. Cleland. The HCl was removed first by adding dry Tris base until the solution was weakly alkaline and then by performing a two-bulb distillation. To determine the ratio of ^{16}O to ^{18}O, approximately 0.5 mg of PCl_5 was quenched in 40 μL of the ^{18}O-enriched water. The resulting HCl was neutralized with an excess of solid imidazole, and the ^{31}P NMR spectrum was obtained in 500 μL of D_2O. The relative abundance of ^{16}O and ^{18}O in phosphate was determined by integrating the five peaks of the phosphate signal [centered at 2.1 ppm; 0.021 ppm separation (*10*); the peaks, from downfield to upfield, correspond to 0−4 atoms of ^{18}O in phosphate] with the program Peakfit (SPSS Inc.). The percentage enrichment of ^{18}O was found to be 78%.

Exchange Reactions. Three 100 μL reaction mixtures were assembled, each containing 1 mM dTDP-glucose-d_7, 1 mM DTT, 1 mg/mL BSA (fraction V), 10 mM ammonium acetate, [^{18}O]water, and 1.8, 24.7, or 14.7 μM wt, D135A, or D135N 4,6-dehydratase, respectively. All of the reagents (except for the [^{18}O]water) were carefully adjusted to pH 7.5 prior to mixing. Each tube contained minimal amounts of components dissolved in natural abundance H_2O that contribute to the ultimate isotopic dilution of ^{18}O. The final percentage of [^{18}O]water in the wt, D135A, and D135N reaction mixtures was 72% in each case. Reactions were initiated at 18 °C by addition of enzyme. For analysis, MALDI-TOF MS samples were prepared by quenching 10 μL aliquots of each reaction, at various times, in 100 μL of 70 °C ethanol (*8*). Precipitated protein was removed by centrifugation, and the ethanolic supernatant was concentrated to dryness in a speed-vac concentrator (Savant) at room temperature. The dried residue was dissolved in 6 μL of H_2O and subjected to MALDI-TOF mass spectrometric analysis.

Data Processing. Mass spectral peak areas were obtained using the program Peakfit (SPSS). The substrate dTDP-glucose-d_7 (monoisotopic mass 571.2, detected in the negative ion mode [M − H] at 570.2) displayed an isotopic envelope consisting of four peaks with 2.3% of the area at m/z = 569.2, 72.1% at m/z = 570.2, 17.8% at m/z = 571.2, and 7.8% at m/z = 572.2 (errors are ~±0.1%). The 569.2 peak was present because the glucose-d_7 used in the synthesis of dTDP-glucose-d_7 contained only 98% deuterium enrichment; the 571.2 and 572.2 peaks were due to the natural abundance of ^{13}C throughout the molecule. Identical isotopic envelopes are assumed for the C5(D) and C6(^{18}OH) exchanged dTDP-glucose species. The relative amounts of each of the four possible exchanged substrate species (dTDP-[6-^{16}O]glucose-d_7, dTDP-[6-^{18}O]glucose-d_7, dTDP-[6-^{16}O]glu-

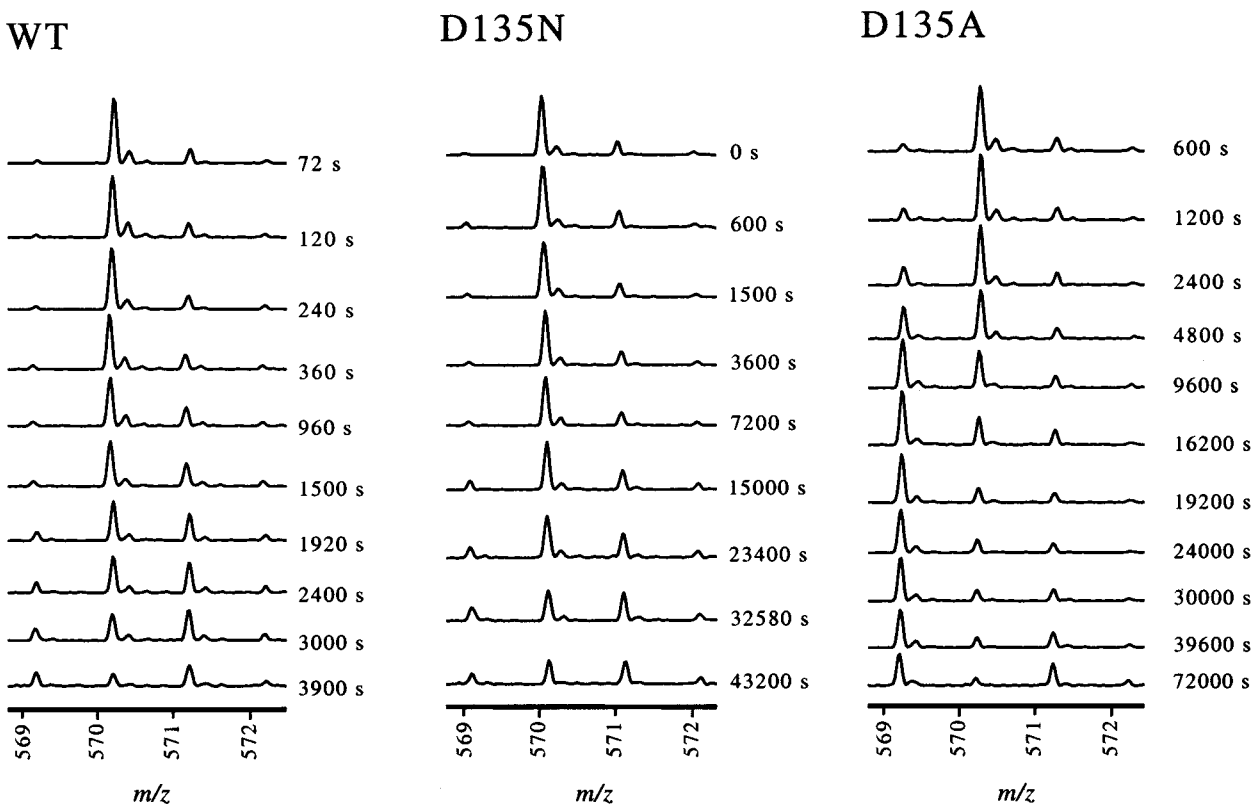

FIGURE 1: Representative mass spectral data for time courses of exchange. Data are exchange reactions catalyzed by wt, D135N, and D135A 4,6-dehydratases. Raw MALDI-TOF mass spectra of timed and quenched samples from exchange reactions with wt, D135N, and D135A are displayed with the time coordinate listed to the right of each spectrum. The mass range (m/z = 569−572) shows all of the various isotopically exchanged forms of dTDP-glucose present in these reactions. The formation of dTDP-4-keto-6-deoxyglucose-d_6 (the only form of product generated in these reactions) was monitored at m/z = 551 and is not shown in these spectra. The time zero spectrum is shown with the D135N reaction and is identical for all three reactions (this gives the isotopic envelope for the dTDP-glucose-d_7 starting material). Spectral data are corrected in two ways to give the subsequent progress curves. First, the overlapping isotopic envelopes are deconvoluted to yield the quantity of each isotopically exchanged form of substrate. Second, the quantities of dTDP-glucose-d_6-C6^{16}O and dTDP-glucose-d_6-C6^{18}O are adjusted to correct for only 72% ^{18}O solvent enrichment in each reaction. Both corrections are detailed in Experimental Procedures. The species at m/z 569 accumulating with time in the wt and D135N reactions is due to the presence of 28% ^{16}O in the [^{18}O]H_2O and appears at the expense of the species at m/z 571. In the wt reaction, correction for ^{16}O in [^{18}O]H_2O, as described in Experimental Procedures, eliminates this species. In the reaction of D135A the m/z 569 species arises mainly from faster exchange of the C5(D) than the C6(OH) owing to the stepwise mechanism followed by the mutated enzyme.

cose-d_6, and dTDP-[6-^{18}O]glucose-d_6) were obtained from the solution to the system of four algebraic expressions:

(1) area of 569.2 peak = 72.1% (dTDP-[6-^{16}O]glucose-d_6) + 2.3% (dTDP-[6-^{16}O]glucose-d_7)

(2) area of 570.2 peak = 17.8% (dTDP-[6-^{16}O]glucose-d_6) + 72.1% (dTDP-[6-^{16}O]glucose-d_7) + 2.3% (dTDP-[6-^{18}O]glucose-d_6)

(3) area of 571.2 peak = 7.8% (dTDP-[6-^{16}O]glucose-d_6) + 17.8% (dTDP-[6-^{16}O]glucose-d_7) + 72.1% (dTDP-[6-^{18}O]glucose-d_6) + 2.3% (dTDP-[6-^{18}O]glucose-d_7)

(4) area of 572.2 peak = 7.8% (dTDP-[6-^{16}O]glucose-d_7) + 17.8% (dTDP-[6-^{18}O]glucose-d_6) + 72.1% (dTDP-[6-^{18}O]glucose-d_7)

As little or no signal was detectable at m/z = 568.2, 573.2, 574.2, and 575.2 expressions were not derived for these masses. The concentration of each species in a given sample was then calculated using the total areas for the isotopic envelope of product (major peak at m/z = 551.2) and deconvoluted substrate species normalized to the starting concentration of 1 mM. Assuming an insignificant ^{18}O isotope effect for the C6(OH) exchange reaction, it is possible to correct for partial solvent ^{18}O enrichment. To make this correction, the [dTDP-[6-^{18}O]glucose-d_6] was divided by the fraction of ^{18}O in each reaction (0.72 in each case as measured above), and the increase was subtracted from the experimentally observed [dTDP-[6-^{16}O]glucose-d_6].

RESULTS

The rates of glucosyl C5(D) solvent hydrogen and C6(OH) solvent oxygen exchange into the substrate were simultaneously determined by mass spectrometric characterization during the multiple turnover conversion of dTDP-glucose-d_7 to product by wt, D135N, and D135A 4,6-dehydratase, in ^{18}O-enriched water. Representative mass spectra, showing the complete set of substrate peaks for wt and D135A reactions, are presented in Figure 1. It is obvious from these raw data that different exchange properties are manifested in the reactions of wt and D135A dehydratases. The relative abundance of substrate and product molecules

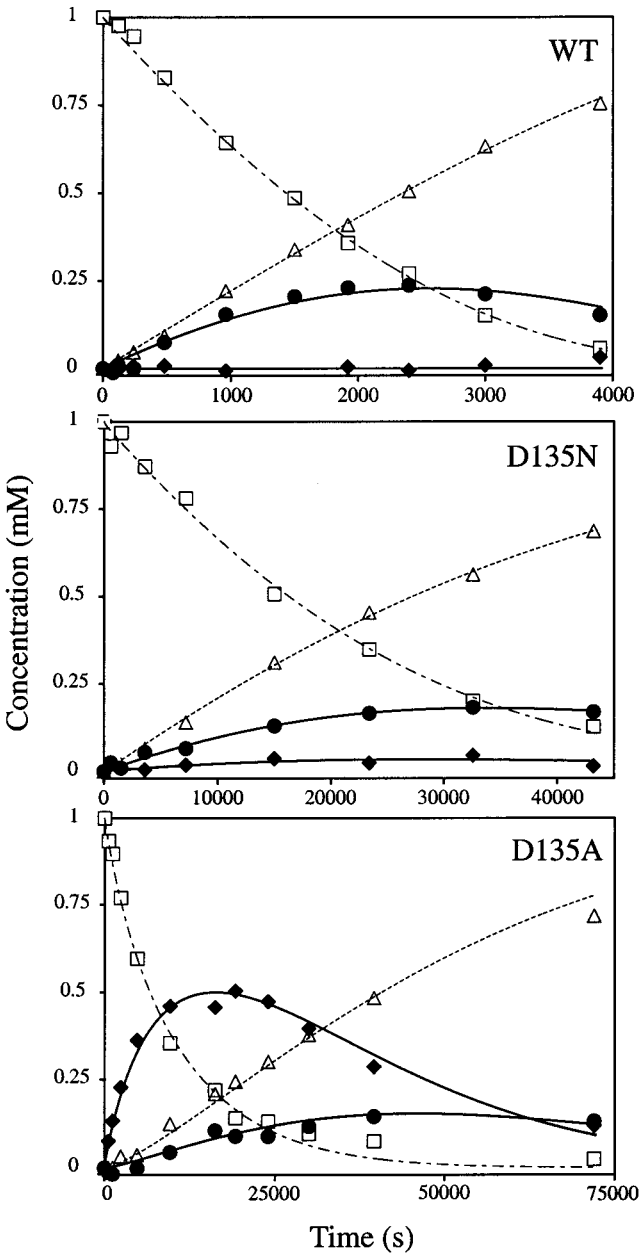

FIGURE 2: Progress curves for exchange of substrate C5(D) and C6(OH) by wt, D135N, and D135A 4,6-dehydratase. The concentrations of dTDP-glucose-d_7-C6^{16}O (□), dTDP-glucose-d_6-C6^{16}O (◆), dTDP-glucose-d_6-C6^{18}O (●), and dTDP-4-keto-6-deoxyglucose-d_6 (△) are plotted at various times for wt, D135N, and D135A exchange reactions. dTDP-glucose-d_7-C6^{18}O did not accumulate in any of the reactions. Curves for each species in each reaction were derived as data were fitted to a minimal kinetic mechanism using the program Dynafit (*11*).

was determined by integration of the MS data, deconvolution of overlapping isotopic envelopes, and correction for fractional ^{18}O enrichment, as described in Experimental Procedures. The resulting data were plotted in Figure 2 for all three reactions. These time courses show the depletion of dTDP-glucose-d_7, production of dTDP-4-keto-6-deoxyglucose-d_6, and the transient formation of dTDP-[6-^{18}O]glucose-d_6. As expected, none of the reactions showed accumulation of dTDP-[6-^{18}O]glucose-d_7, which would only form if elimination occurred by way of a primary carbocation intermediate. Biological elimination reactions usually occur by E1cb or concerted (E2-like) mechanisms and not by E1 mechanisms. Biological reactions with carbocationic intermediates are not observed, except in cases of allylic stabilization of the carbocation, as in polyterpene cyclases, and glycosyl transfer reactions through oxocarbenium ion intermediates.

The major qualitative difference among the three progress curves in Figure 2 is the rate of formation and accumulation of substrate with the C5 solvent hydrogen exchanged that has not also acquired ^{18}O, that is, dTDP-[6-^{16}O]glucose-d_6. The reaction of wt dehydratase shows no accumulation of dTDP-[6-^{16}O]glucose-d_6, only the transient accumulation of doubly exchanged substrate (dTDP-[6-^{18}O]glucose-d_6). In contrast, the reaction of D135A dehydratase shows a rapid burst of C5 solvent hydrogen exchanged substrate (dTDP-[6-^{16}O]glucose-d_6) preceding the slower transient formation of doubly exchanged substrate (dTDP-[6-^{18}O]glucose-d_6). Unlike the wt enzyme, the D135N dehydratase allows some singly exchanged substrate to accumulate but does not show the same rapid burst of proton exchange catalyzed by D135A.

To enable quantitative interpretation of our exchange results, all three sets of progress curves were fitted to a comprehensive minimal kinetic model shown in Figure 3. In this model dTDP-glucose-d_7 may be depleted through one or both of two irreversible steps. The first (k_1) leads directly to C5 solvent hydrogen exchanged substrate (dTDP-[6-^{16}O]-glucose-d_6) and requires dehydrogenation to the 4-ketone, 5-enolization, enzyme−base solvent hydrogen exchange, and re-formation of substrate. The second (k_3) leads to a common intermediate, **I**, which must be the dTDP-4-ketoglucose-5,6-ene as it lacks both the C5(H) and the C6(OH) but is capable of reacting with water in the active site in reverting to the substrate. Because the reaction was carried out in [^{18}O]water, re-formation of substrate from **I** can only generate dTDP-[6-^{18}O]glucose-d_6. This process was modeled as a reversible step (k_5, k_6). The reincorporation of ^{16}O into **I**, yielding the other two substrate forms (dTDP-[6-^{16}O]glucose-d_7 and dTDP-[6-^{16}O]glucose-d_6), is disallowed because of isotopic dilution of ^{16}O. These steps were modeled as irreversible (k_3, k_5). The same rate constant (k_5) was used for the forward reaction of both C5 protonated substrates, as experimental error will be of the same or larger magnitude as the ^{18}O isotope effect. Transformation of **I** into product was modeled with an irreversible step (k_7).

At first glance, analysis of the reaction might appear to be subject to simplification by steady-state approximations. Because substrate is in excess of enzyme (1 mM dTDP-[6-^{16}O]glucose-d_7; wt, D135A, and D135N are 1.8−24.7 μM) and the isotopically exchanged forms of substrate (dTDP-[6-^{16}O]glucose-d_6 and dTDP-[6-^{18}O]glucose-d_6) are diluted into a large pool of dTDP-[6-^{16}O]glucose-d_7, the reaction can only be accurately described using a series of differential equations. As the reaction progresses, the product and substrate will compete for the enzyme. For these reasons substrate and product binding steps (k_{on}, k_{off}) were included in the differential kinetic model. Although K_D for the substrate has not been determined, its value can be estimated from other constants. The K_M is 5 μM (*9*). The substrate analogue dTDP-xylose binds wt 4,6-dehydratase with a K_D of 7 μM, and the product binds with a K_D of 25 μM (*5*). For the purposes of modeling the exchange reactions the value of K_D for the substrate was assumed to be 10 μM. Equilibrium binding was also assumed with k_{on} being fixed at

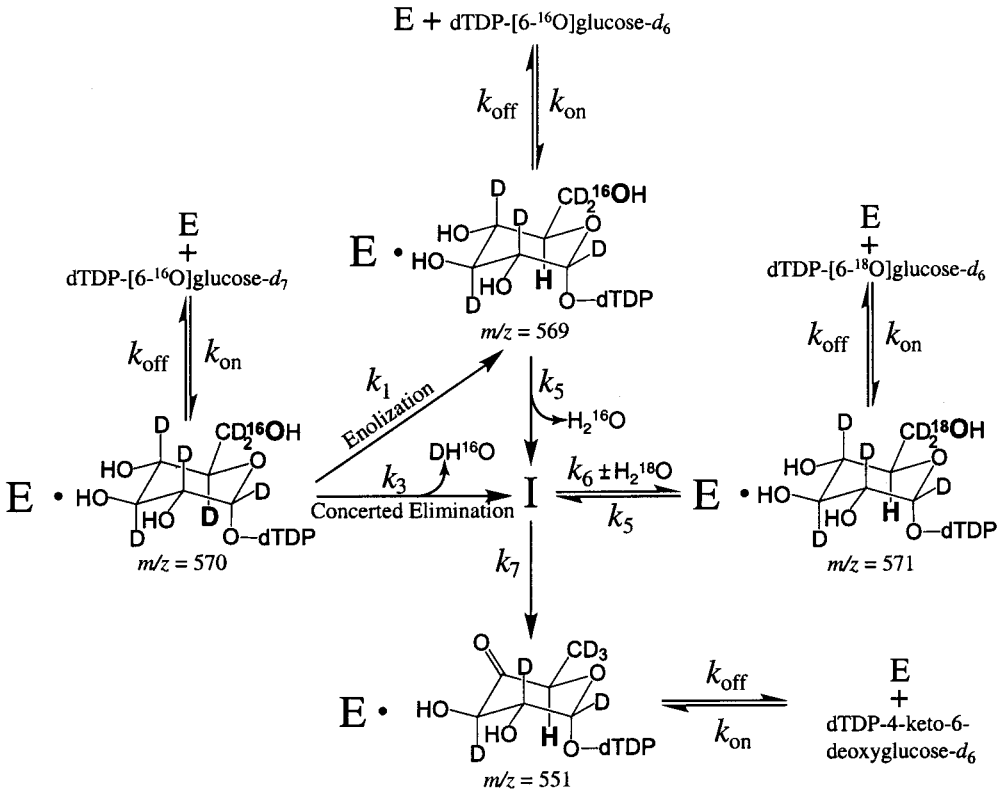

FIGURE 3: Kinetic mechanism for the action of 4,6-dehydratase. This is the minimal kinetic mechanism used to fit all three data sets shown in Figure 2. Steps indicated by k_1, k_3, and k_5 are irreversible because of infinite dilution of exchanged $DH^{16}O$ and $H_2{}^{16}O$ into solvent $H_2{}^{18}O$. Listed *m*/*z* values are for the monoanionic (M − H) nucleotide sugar species as detected during negative ion mode MALDI-TOF mass spectrometric analysis. Intermediate **I** is included in this model to provide appropriate connectivity between detectable nucleotide sugar species. From previous studies (*8*), **I** will predominantly be dTDP-4-ketoglucose-5,6-ene, but since enzyme concentrations are very low compared to dTDP-glucose, **I** is undetectable.

1000000 M^{-1} s^{-1} (approximately $k_{cat}/K_M = 820000$ M^{-1} s^{-1}; *9*) and k_{off} at 10 s^{-1} (consistent with $K_D \sim 10$ μM). Binding isotope effects were assumed to be insignificant for the present purposes, and identical k_{on} and k_{off} values were used for all three substrate species. Values for k_{on} and k_{off} were 1000000 M^{-1} s^{-1} and 10 s^{-1} for wt and 100000 M^{-1} s^{-1} and 1 s^{-1} for D135N and D135A. The fitting program, Dynafit (*11*), did not converge with slower k_{on} and k_{off} for wt or faster k_{on} and k_{off} for the reaction of D135N. The data for D135A were fitted with either set of k_{on} and k_{off} values with negligible effects on the fitted parameters. The progress curve fits are shown as solid and dashed lines in Figure 4, and the kinetic parameters derived from these fits are listed in Table 1.

The failure of dTDP-glucose-d_6-C6^{16}O to accumulate in the wt progress curves makes it impossible to derive a value for k_1, indicating that $k_1 \ll k_3$. The large differences in rate constants between wt and the Asp135 variants are not apparent in Figure 2 because of differences in enzyme concentration and time domains. In each case the major contributor to overall rate limitation in product formation is k_7. The published decrements in k_{cat} for D135N and D135A compared with wt k_{cat} (124- and 223-fold, respectively) are consistent with the 50- and 107-fold decreases observed for k_7, requiring only an additional 2-fold contribution from other steps. All of the other constants in the Asp135 variant reactions have suffered major decrements, the largest being for k_3 in the reaction of D135A, which is nearly 5000-fold below the wt value. The value of k_3 for D135N dehydratase is only 400-fold below the wt value.

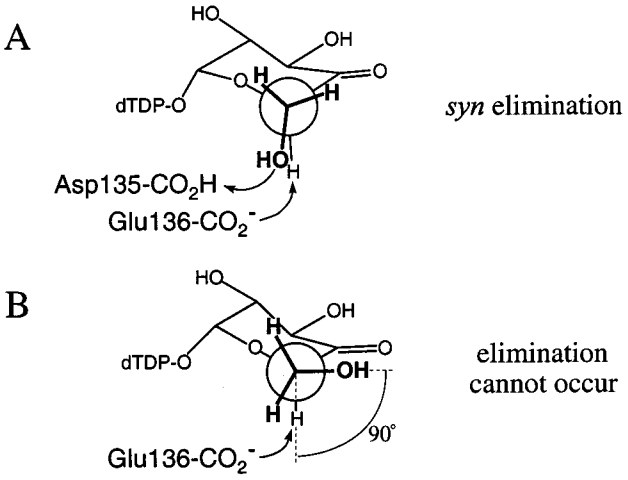

FIGURE 4: Effects of C5−C6 bond rotomeric configuration on chemistry. Newman projections through the C5−C6 bond show the importance of rotomeric conformation to elimination chemistry. In panel A, the configuration is optimal for the concerted *syn* elimination. In panel B, elimination cannot occur as a result of insufficient orbital overlap; deprotonation of C5 results in delocalization of the nascent carbanion into the adjacent ketone functionality (enolization).

Both water elimination and enolization are initiated by C5H/D abstraction. To judge the extent of the effects of the mutation of Asp135 on dehydration, it is valuable to compare the sum of the rate constants for enolization (k_1) and concerted elimination (k_3) to the wt k_3. Quite remarkably, $k_1 + k_3$ (listed in Table 1) values are very similar for the D135A and D135N dehydratases and are 370-fold lower than k_3 for

Table 1: Kinetic Parameters Derived from Steady-State Exchange Progress Curves[a]

	wt rate (s^{-1})	D135A rate (s^{-1})	D135N rate (s^{-1})
k_1	—[b]	0.0053 (±0.0006)	0.0004 (±0.0001)
k_3	2.1 (±0.8)	0.0004 (±0.0002)	0.005 (±0.0008)
k_5	1.5 (±0.7)	0.0022 (±0.0003)	0.004 (±0.0009)
k_6	0.13 (±0.01)	0.0008 (±0.0003)	0.001 (±0.0003)
k_7	0.15 (±0.01)	0.0014 (±0.0004)	0.003 (±0.0005)
$k_1 + k_3$[c]	2.1 (±0.8)	0.0057 (±0.0008)	0.0054 (±0.0009)
$k_1/(k_1 + k_3)$[d]	0.0	0.9 (±0.2)	0.07 (±0.02)

[a] Rate constants were obtained using the kinetic mechanism shown in Figure 3 and the fitting program Dynafit (*11*). [b] The rate constant k_1 in wt consistently approached a meaninglessly small number with a large error as the other rate constants converged. This step could be removed from the kinetic mechanism used to fit the wt data without affecting the values of the other constants. [c] This expression corresponds to the rate of dTDP-glucose-d_7 depletion. [d] This ratio is the fraction of dTDP-glucose-d_7 that enolizes rather than eliminating water.

wt dehydratase. Obviously the 360-fold decrease may not fully reflect the extent of the drop in rate of water elimination, as k_3 refers to the net forward rate through the fully reversible 4-dehydrogenation and the irreversible [^{16}O]water elimination. The ratio of k_1 and $k_1 + k_3$ (values listed in Table 1) describes the partitioning between enolization and concerted elimination. This coefficient indicates the fraction of dTDP-[6-^{16}O]glucose-d_7 that is depleted by enolization. For D135A, D135N, and wt 4,6-dehydratase these values are 0.9, 0.07, and 0.0, respectively. The large differences in these fractions from D135N to D135A despite similar values of $k_1 + k_3$ clearly indicate that the increased occurrence of enolization is not simply due to removal of acid catalysis but must have a more fundamental mechanistic basis. This issue will be dealt with extensively below.

DISCUSSION

The primary objective of this study is to determine whether wt 4,6-dehydratase catalyzes the dehydration of dTDP-4-ketoglucose to dTDP-4-ketoglucose-5,6-ene through a stepwise (Scheme 2), or concerted (Scheme 1), elimination of water. By simultaneous kinetic analysis of C5(D) solvent hydrogen and C6(OH) solvent oxygen exchange into substrate, dehydration appears to proceed through the concerted elimination mechanism. Interestingly, variants of active site amino acid residue Asp135 alter the dehydration mechanism so that elimination occurs through the stepwise mechanism. The D135N and D135A dehydratases display distinctly different partitioning between concerted elimination and stepwise elimination pathways, albeit at much slower rates, allowing sensible speculation on the physical basis for the control of this partitioning (below).

Clearly our mechanistic interpretations of concurrent exchange of C5(D) and C6(OH) rely on the exchange of protons and the release of water molecules from the enzyme active site at rates exceeding that of elimination chemistry. The direct observation of concerted and stepwise mechanisms in wt and variant dehydratases, respectively, demonstrates the rapidity with which protons and oxygen exchange with solvent, at least within the context of the slower reactions of Asp135 variants. For the much faster wt-catalyzed exchange reaction, we know that in the overall reaction the C5(H) exchanges much faster than turnover k_{cat} (5 s^{-1}) because of the 100% incorporation of deuterium at C5 in the product generated in D_2O (*3*, *7*). While one might be concerned that the eliminated water molecule could be retained in the wt active site, the absence of accumulating dTDP-[6-^{16}O]glucose-d_6 in the wt profile shows that water is readily released from the active site.

The essential facts about the kinetics of the elimination reaction are as follows: (a) The solvent exchanges of C5-(D) for H and C6(OH) for ^{18}OH in the substrate occur at the same rate. No difference can be detected. The simplest interpretation of this fact is that the dehydration proceeds in a concerted step, as shown in Scheme 1. (b) A more complex interpretation would be that the elimination is stepwise as in Scheme 2, where the rate constant for elimination of C6-(OH) from the enol(ate) is larger that the rate constant for enol(ate) formation. Then, no enol(ate) would accumulate, as previously reported (*8*), and the solvent exchange of C5-(D) would occur before reverse addition of water to the dTDP-4-ketoglucose-5,6-ene. According to this interpretation, a slowing of the elimination step in Scheme 2 would allow the buildup of dTDP-4-ketoglucose, and its enolization and solvent exchange of C5(D) would then be observed. One way to slow the second step is to abolish the elimination through the substitution of dTDP-D-xylose for dTDP-glucose. In earlier studies (*5*, *9*) we examined the reaction of dTDP-D-xylose and solvent exchange of C5(H). dTDP-D-xylose at the active site rapidly undergoes the dehydogenation by NAD^+ ($k = 1$ s^{-1}) to 73% dTDP-4-ketoxylose and NADH at equilibrium. Thus, the C5(H) is activated for enolization, but the pseudointermediate cannot undergo either the overall reaction or the elimination of water. Despite the fact that the pseudointermediate builds to 73% in the active site, wild-type 4,6-dehydratase catalyzes the C5(H,D) exchange with a rate constant of only 0.001 s^{-1} and for D135A 0.002 s^{-1}. These exchange rate constants are many orders of magnitude lower than k_{cat} for the overall reaction (5 s^{-1}) and many orders of magnitude slower than the rehydration and reduction of dTDP-4-ketoglucose-5,6-ene ($k = 3$ s^{-1}) to dTDP-glucose (*8*). The essential absence of solvent exchange cannot be attributed to a forward commitment in this case. The simplest interpretation of all the results is that abstraction of the C5(H,D) from dTDP-4-ketoglucose is mechanistically connected to the elimination of C6(OH).

It is difficult to envision a scenario where net C5(H) exchange from the enzyme active site occurs rapidly from the 4,6-dehydratase/dTDP-4-ketoglucose-5,6-ene complex but several orders of magnitude more slowly from the 4,6-dehydratase/dTDP-4-ketoglucose-5-enol(ate) complex. Under this scenario the wt reaction would appear to be concerted, with equal C5(H) and C6(OH) exchange rates, but could proceed by either stepwise or concerted mechanisms. In this scenario Glu136-COOH exchanges rapidly with solvent in the intermediate with dTDP-4-ketoglucose-5,6-ene but not in the intermediate with dTDP-4-ketoglucose-5-enol(ate). While one might imagine that the two enzyme intermediate complexes could have radically different exchange properties, this extreme case seems unlikely once the significantly slower reactions of the Asp135 variants are examined. The D135N reaction proceeds with nearly identical C5(H) and C6(OH) exchange rates, meaning that the slow exchange from the enol(ate) complex is significantly (another 2 orders of magnitude) slower than was needed to make a stepwise wt reaction appear concerted, yet D135A allows rapid solvent

Scheme 3

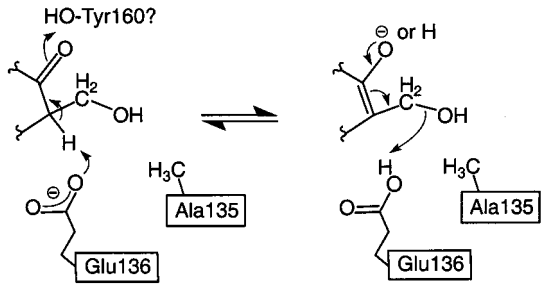

hydrogen exchange from the same complex. This scenario is more complex and less reasonable than the concerted mechanism, given the large differences in 4,6-dehydratase/dTDP-4-ketoglucose-5,6-ene vs 4,6-dehydratase/dTDP-4-ketoglucose-5-enol(ate) exchange rates needed to explain the wt and D135N results and the large increase in the 4,6-dehydratase/dTDP-4-ketoglucose-5-enol(ate) exchange rate caused by the D135A variant.

Available facts do not support a stepwise mechanism but are consistent with a concerted mechanism. Deletion of the acid catalyst in D135N and especially D135A dramatically lowers the rate and, as is typical in such studies with enzymes, allows a different, in this case, stepwise, mechanism to take over.

Both Asp135 variants show significantly lower values of all five rate constants, k_1, k_3, k_5, k_6, and k_7, relative to wt. The circular dichroism spectra of wt, D135N, and D135A are indistinguishable, so significant changes in secondary structure are not responsible for the lower values (*9*). One would expect k_1, k_3, k_5, and k_6 to be affected by changes in catalysis of dehydration and thus be susceptible to variation of Asp135 and/or Glu136. It is perhaps less obvious why variation of Asp135 would affect k_7, as this constant solely governs the rate for the irreversible reduction of the intermediate dTDP-4-keto-glucose-5,6-ene (**I**) to the product dTDP-4-keto-6-deoxyglucose. The ~100-fold lower value of k_7 indicates that mutation of Asp135 is somehow harming the catalysis of rereduction. One possibility is that the Asp135 variants are altering the ability of Glu136 to function as the acid catalyst. With the alteration of Asp135, acid catalysis of water elimination may be accomplished by another active site amino acid residue, potentially Glu136. This scenario would leave Glu136 in the wrong protonation state (deprotonated) for the reduction step. Conceivably, both base and acid catalysis by Glu136 could occur by the mechanism shown in Scheme 3. Given the observed rapidity of solvent hydrogen exchange from Glu136, prototrophic rate limitation for the following step is unlikely (*5*). Alternatively, one might expect significant changes in the acid/base properties of Glu136 to result from the removal of the adjacent Asp135 carboxylic acid functionality. These two residues probably function together in the active site to promote net catalysis efficiently. The Asp135 variants may also have other effects on the reduction step that we cannot yet describe in detail.

Differences between the kinetics and means of substrate depletion by wt, D135N, and D135A suggest multiple functions for Asp135. While both D135N and D135A show similar rates of substrate depletion ($k_1 + k_3$), D135A, D135N, and wt 4,6-dehydratases show large differences in the partitioning between enolization and concerted dehydration [$k_1/(k_1 + k_3)$]. The lower rates of substrate depletion for the two Asp135 variants (370-fold slower than that for wt) may be largely due to the removal of the acid catalyst for dehydration. It is possible that the lower rates are caused by the partial incapacitation of Glu136, which will become a weaker base once the adjacent Asp135 acid functionality is removed.

By functioning in concert, Asp135 and Glu136 catalyze water elimination in a manner that does not necessitate formation of a high energy intermediate. Removal of either the acid or base would force the reaction through a higher energy transition state and would slow the rate as the $\Delta\Delta G^{\circ\ddagger}$ is made larger. Enolization leads to the higher energy carbanionic intermediate with delocalization of the nascent negative charge at C5 into the 4-keto functionality. In the action of the wt 4,6-dehydratase, where concerted acid/base dehydration catalysis is maintained, enolization cannot contribute further to transition state stabilization and occurs too slowly to be observed in the presence of the more energetically favorable concerted reaction.

The large observed difference in partitioning between enolization and concerted elimination by D135N and D135A forces one to consider how small structural differences between these variants might guide the reaction through one or the other pathway. One way that the different partitioning may be explained is by invoking an increase in rotational freedom about the C5−C6 bond resulting from alterations in hydrogen-bonding potential as Asp135 is changed to asparagine and alanine. The stereochemical course of the dehydration reaction has been shown to be *syn*, as depicted in a Newman projection in Figure 4A (*6*). It is reasonable to propose that Asp135, as the acid catalyst for water elimination, also donates a hydrogen bond to the C6(OH). This hydrogen-bonding interaction may be important in preventing the C6(OH) from assuming rotational conformations that are suboptimal for elimination, as would be the case as the C6-(OH) approaches a position orthogonal to the C5(H) (Figure 4B). Loss of control over rotational freedom would likely favor enolization, as productive orbital overlap for elimination would be less frequent at best and disfavored at worst. As depicted in Figure 5, wt and D135N are capable of asserting this rotational control through hydrogen-bonding interactions, while D135A is not. It is also possible that nonproductive C5−C6 bond rotational conformers are excluded by steric means, although given Asp135's role in acid catalysis, hydrogen bonding is probably also involved.

Other 4,6-dehydratases, like GDP-mannose 4,6-dehydratase and CDP-glucose 4,6-dehydratase, might contain analogous active site amino acid configurations to promote concerted acid/base catalysis of dehydration and to control C5−C6 bond rotation. The crystal structure of GDP-mannose 4,6-dehydratase (PDB 1DB3) shows a glutamate residue, analogous to Glu136, that has been identified as the base that deprotonates C5, but a serine residue is in place of Asp135 (*12*). It is possible that some other residue may provide acid catalysis, although it is hard to speculate what that residue might be given that the structure does not contain GDP-mannose. Amino acid sequence alignments show that conserved lysine and aspartate residues from the CDP-glucose 4,6-dehydratase correspond to the Glu136 and Asp135 from dTDP-glucose 4,6-dehydratase, although no

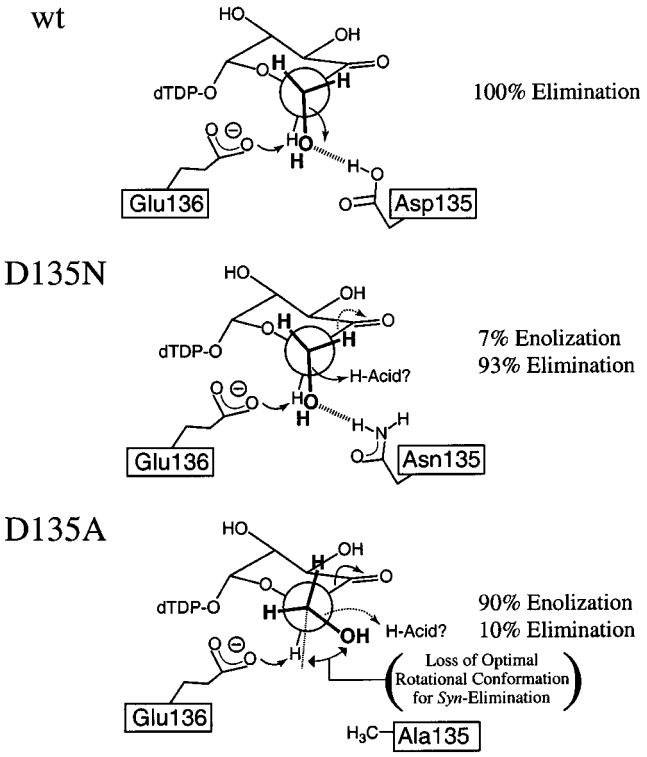

FIGURE 5: Enolization and concerted water elimination in wt, D135N, and D135A. Three panels postulate mechanistic explanations for the observed exchange results of wt, D135N, and D135A. The partitioning between enolization and elimination is indicated in each panel. Dotted arrows represent a less frequent electronic motion. In the wt reaction a hydrogen bond locks the C6(OH) into position for a concerted acid/base-catalyzed *syn* elimination. The D135N variant can still provide a hydrogen-bonding interaction with the C6(OH), but it cannot function as an acid catalyst. As a result the elimination is slowed, but enolization only occurs during 7% of substrate depletion. The D135A variant is incapable of both hydrogen bonding and acid catalytic functions, and thus the reaction is slowed, and enolization occurs 90% of the time.

structural data are available to confirm these assignments (*13*).

Gerlt and Gassman described concerted acid/base catalysis of enolization as a means of explaining rapid catalytic turnover of β-elimination reactions despite large pK_a gaps between the substrate α-carbon acids and the active site bases (*2*). Kinetic isotope effect studies of enoyl-CoA hydratase (crotonase) indicate that it catalyzes a concerted hydration at the β-position of an α-β unsaturated thioester (*14*, *15*). Enoyl-CoA hydratase has other similarities to 4,6-dehydratase in that it employs two carboxylic acid amino acid active site residues, Glu144 and Glu164 (analogous to Glu136 and Asp135, respectively, in 4,6-dehydratase), for acid/base catalysis of a concerted *syn* hydration (*16*). Gerlt and Gassman concede that concerted acid/base catalysis of β-elimination reactions would resolve similar pK_a discrepancies in dehydration reactions without necessitating the formation of an enol intermediate (*2*). Concerted acid/base catalysis of either elimination or enolization may be employed in enzyme-catalyzed reactions to decrease energy barriers in cases where large pK_a differences exist between active site residues and substrates.

ACKNOWLEDGMENT

We thank Professor W. W. Cleland for the generous gift of the [^{18}O]water. MALDI-TOF spectra were obtained at the University of Wisconsin−Madison Biophysics Instrumentation Facility, which is supported by the University of Wisconsin−Madison and Grants BIR-9512577 (NSF) and S10 RR13790 (NIH).

REFERENCES

1. . March, J. (1985) Acids and bases in *Advanced Organic Chemistry*, 3rd ed., pp 218−236, John Wiley and Sons, New York.
2. .Gerlt, J. A., and Gassman, P. G. (1992) *J. Am. Chem. Soc. 114*, 5928−5934.
3. .Gabriel, O., and Lindquist, L. C. (1968) *J. Biol. Chem. 243*, 1479−1484.
4. .Allard, S. T. M., Giraud, M.-F., Whitfield, C., Graninger, M., Messner, P., and Naismith, J. H. (2001) *J. Mol. Biol. 307*, 283−295.
5. .Gross, J. W., Hegeman, A. D., Gerratana, B., and Frey, P. A. (2001) *Biochemistry* (in press).
6. .Snipes, C. E., Brillinger, G. U., Sellers, L., Mascaro, L., and Floss, H. G. (1977) *J. Biol. Chem. 252*, 8113−8117.
7. .Melo, A., and Glaser, L. (1968) *J. Biol. Chem. 243*, 1475−1478.
8. . Gross, J. W., Hegeman, A. D., Vestling, M. M., and Frey, P. A. (2000) *Biochemistry 39*, 13633−13640.
9. .Hegeman, A. D., Gross, J. W., and Frey, P. A. (2001) *Biochemistry 40*, 6598−6610.
10. .Cohn, M., and Hu, A. (1978) *Proc. Natl. Acad. Sci. U.S.A. 75*, 200−203.
11. .Kuzmic, P. (1996) *Anal. Biochem. 237*, 260−273.
12. .Somoza, J. R., Menon, S., Schmidt, H., Joseph-McCarthy, D., Dessen, A., Stahl, M. L., Somers, W. S., and Sullivan, F. X. (2000) *Structure 8*, 123−135.
13. .He, X., Thorson, J. S., and Liu, H.-w. (1996) *Biochemistry 35*, 4721−4731.
14. .Bahnson, B. J., and Anderson, V. E. (1989) *Biochemistry 28*, 4173−4181.
15. .Bahnson, B. J., and Anderson, V. E. (1991) *Biochemistry 30*, 5894−5906.
16. .Hofstein, H. A., Feng, Y., Anderson, V. E., and Tonge, P. J. (1999) *Biochemistry 38*, 9508−9516.

BI011748C